Organic & Biomolecular Chemistry

PAPER

Manadoperoxides, a new class of potent antitrypanosomal agents of marine origin†

Giuseppina Chianese,[a] **Ernesto Fattorusso,**[a] **Fernando Scala,**[a] **Roberta Teta,**[a] **Barbara Calcinai,**[b] **Giorgio Bavestrello,**[c] **Henny A. Dien,**[d] **Marcel Kaiser,**[e,f] **Deniz Tasdemir**[g] **and Orazio Taglialatela-Scafati***[a]

Chemical investigation of the marine sponge *Plakortis* cfr. *lita* afforded a library of endoperoxyketal polyketides, manadoperoxides B–K (**3–5** and **7–13**) and peroxyplakoric esters B₃ (**6**) and C (**14**). Eight of these metabolites are new compounds and some contain an unprecedented chlorine-bearing THF-type ring in the side chain. The library of endoperoxide derivatives was evaluated for *in vitro* activity against *Trypanosoma brucei rhodesiense* and *Leishmania donovani*. Some compounds, such as manadoperoxide B, exhibited ultrapotent trypanocidal activity ($IC_{50} = 3$ ng mL^{-1}) without cytotoxicity. Detailed examination of the antitrypanosomal activity data and comparison with those available in the literature for related dioxane derivatives enabled us to draw a series of structure–activity relationships. Interestingly, it appears that minor structural changes, such as a shift of the methyl group around the dioxane ring, can dramatically affect the antitrypanosomal activity. This information can be valuable to guide the design of optimized antitrypanosomal agents based on the dioxane scaffold.

1. Introduction

African trypanosomiasis (also called sleeping sickness) is a human disease caused by the single-celled protozoan parasites *Trypanosoma brucei gambiense* (in Western and Central Africa) and *T. b. rhodesiense* (in Eastern and Southern Africa) and transmitted to humans by bites of tsetse flies (*Glossina* genus), which have acquired their infection from human beings or from animals harbouring the human pathogenic parasites.[1] Once injected into the humans, trypanosomes multiply in subcutaneous tissues, blood and lymph and, in a second stage, they cross the blood-brain barrier and attack the central nervous system. The process can take years with *T. b. gambiense*, while *T. b. rhodesiense* is responsible for acute infections. When the parasites invade the central nervous system they lead to neurological symptoms, including behavioural changes, coma, and ultimately, if untreated, death. Disturbance of the sleep cycle, which gives the disease its name, is a characteristic feature of this second stage of the disease.

Recent figures have estimated that sleeping sickness threatens at least 60 million people in 36 countries with the number of infections ranging between 50 000 and 70 000 per year, thus qualifying it as the world's third most devastating tropical disease.[2] The rural populations living in regions where transmission occurs and which depend on agriculture, fishing, animal husbandry or hunting are the most exposed to the bite of the tsetse fly and therefore to the disease. Socio-political instability and the consequent population movements, combined with a shortage of funds have largely contributed to determining the recent spread of trypanosomiasis, which, together with other tropical diseases, results in billions of dollars of lost productivity, contributing to determine the poverty and the social isolation of these regions.

Treatment of African trypanosomiasis is still today based on very few molecules, almost all introduced about one century ago. Pentamidine and suramin are the preferred options for the treatment of the first stage, while to treat the second, cerebral stage, eflornithine and the trivalent arsenic derivative melarsoprol are practically the only therapeutic options.[3] Melarsoprol has many disadvantages since it can induce a reactive encephalopathy (encephalopathic syndrome) which can be fatal, while eflornithine is very expensive and ineffective against *T. b. rhodesiense*. Moreover, an increase of cross-resistance to

[a]Dipartimento di Chimica delle Sostanze Naturali, Università di Napoli "Federico II", Via D. Montesano, 49, 80131 Napoli, Italy. E-mail: scatagli@unina.it; Fax: +(0039) 081-678552; Tel: +(0039) 081-678509
[b]Dipartimento di Scienze del Mare, Università Politecnica delle Marche, Via Brecce Bianche, 60131 Ancona, Italy
[c]Dipartimento per lo Studio del Territorio e delle sue Risorse, Università di Genova, Corso Europa 26, 16132 Genova, Italy
[d]Faculty of Fishery and Marine Science, Sam Ratulangi University, Manado, Indonesia
[e]Department of Medical Parasitology and Infection Biology, Swiss Tropical and Public Health Institute, CH-4002 Basel, Switzerland
[f]University of Basel, Petersplatz 1, CH-4003 Basel, Switzerland
[g]School of Chemistry, National University of Ireland, Galway, University Road, Galway, Ireland
†Electronic supplementary information (ESI) available: 1D and 2D NMR spectra for compounds **7–14**. See DOI: 10.1039/c2ob26124c
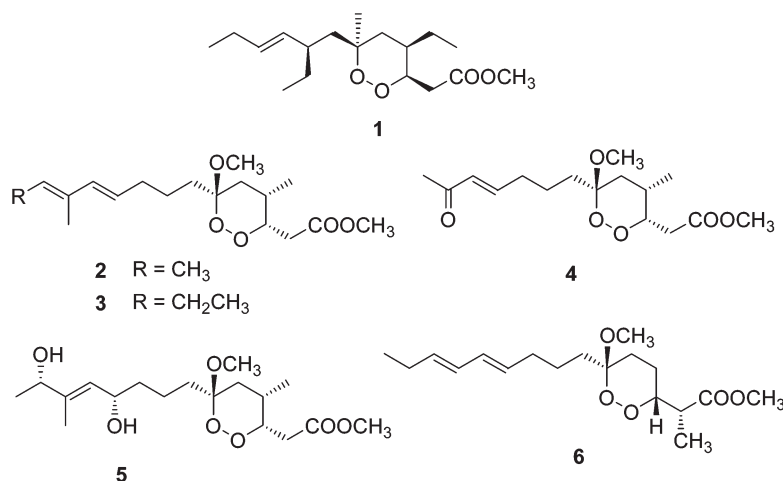
This journal is © The Royal Society of Chemistry 2012

Org. Biomol. Chem., 2012, **10**, 7197–7207 | 7197

Fig. 1 Chemical structures of known compounds: plakortin (**1**), manadoperoxides A–D (**2–5**) and peroxyplakoric ester B₃ (**6**).

these drugs has been observed in recent times, especially in central Africa and, thus, the few available drugs are rapidly losing their effectiveness.[4] In recent years, only one compound, pafuramidine (a synthetic analogue of pentamidine), has been clinically evaluated against African trypanosomiasis, but further development was discontinued in 2008 due to liver toxicity.[5] Recently, the nitroimidazole derivative fexinidazole, bearing structural similarities with metronidazole and nifurtimox, has entered Phase II/III clinical trials[6] and is the most advanced drug candidate against trypanosomiasis. However, there is still an urgent need to find new, effective and, above all, affordable alternatives to the existing options for treatment of sleeping sickness.

We have been actively engaged in the field of tropical disease treatment and discovered that some classes of natural products are endowed with promising activity against *Plasmodium falciparum* and *Leishmania* parasites.[7–9] Among them, plakortin (**1**, Fig. 1), a simple 1,2-dioxane polyketide obtained from the Caribbean sponge *Plakortis simplex*[7] was demonstrated to possess significant *in vitro* antimalarial activity against CQ-resistant *P. falciparum* strains without cellular toxicity.[7] By means of a multidisciplinary approach (including computational and experimental studies) on natural analogues[10,11] and semisynthetic derivatives,[12] we also obtained valuable information about the SARs needed for the antimalarial activity of these simple 1,2-dioxanes. These results clearly indicated the crucial role of the endoperoxide functionality, suggested the importance of the alkyl side chain, and revealed conformation-dependent features critical for antimalarial activity.[13] We recently developed two different synthetic approaches for the preparation of simplified plakortin analogues and some of the prepared compounds succeeded in reaching the *in vitro* antimalarial potency of plakortin.[14,15]

In this context, we have recently reported the results of the chemical investigation of the Indonesian sponge *Plakortis* cfr. *simplex*,[16] which resulted in the isolation of four endoperoxyketal derivatives named manadoperoxides A–D (**2–5**, Fig. 1),[17] These compounds were assayed *in vitro* against CQ-R and CQ-S *P. falciparum* strains and showed relatively poor antimalarial

potency (5–10 μM), more than ten times lower than that exhibited by plakortin (**1**).

As part of our ongoing screening of natural sources to find new antiprotozoal lead compounds, we have undertaken the chemical analysis of the sponge *Plakortis* cfr. *lita* de Laubenfels, a species widely distributed in the Indo-West Pacific,[18] which was collected along the coasts of the Bunaken Marine Park of Manado (North Sulawesi, Indonesia). Careful inspection of the organic extract of this organism afforded the known manadoperoxides B–D (**3–5**) and peroxyplakoric ester B₃ (**6**) (Fig. 1), along with eight new peroxyketal polyketides, which we named manadoperoxides E–K (**7–13**) and peroxyplakoric ester C (**14**) (Fig. 2). Herein we provide details about their isolation, stereostructural determination and SARs, as well as *in vitro* trypanocidal and leishmanicidal effects. The present study provides the first data on the antitrypanosomal activity of endoperoxyketal derivatives.

2. Results

2.1 Chemistry

The sponge *Plakortis* cfr. *lita* de Laubenfels (order Homosclerophorida, family Plakinidae) was collected in January 2010 from along the coasts of Bunaken Island (Manado, Indonesia). After homogenization, the organism was exhaustively extracted sequentially with MeOH and CHCl₃. The combined extracts were subjected to chromatography over reversed-phase silica column eluting with a solvent gradient of decreasing polarity from water to chloroform. Selected fractions were combined and further fractionated by gravity column chromatography (CC) on silica gel, followed by repeated open CC and HPLC (*n*-hexane–EtOAc mixtures) to afford the new polyketide manadoperoxides E–K (**7–13**) and peroxyplakoric ester C (**14**) in the pure state, along with the known manadoperoxides B–D (**3–5**)[17] and peroxyplakoric ester B₃ (**6**).[19] The structures of the known compounds **3–6** were deduced by comparing their spectroscopic data with those previously reported,[17,19] while the structures of the new compounds **7–14** have been deduced as follows.
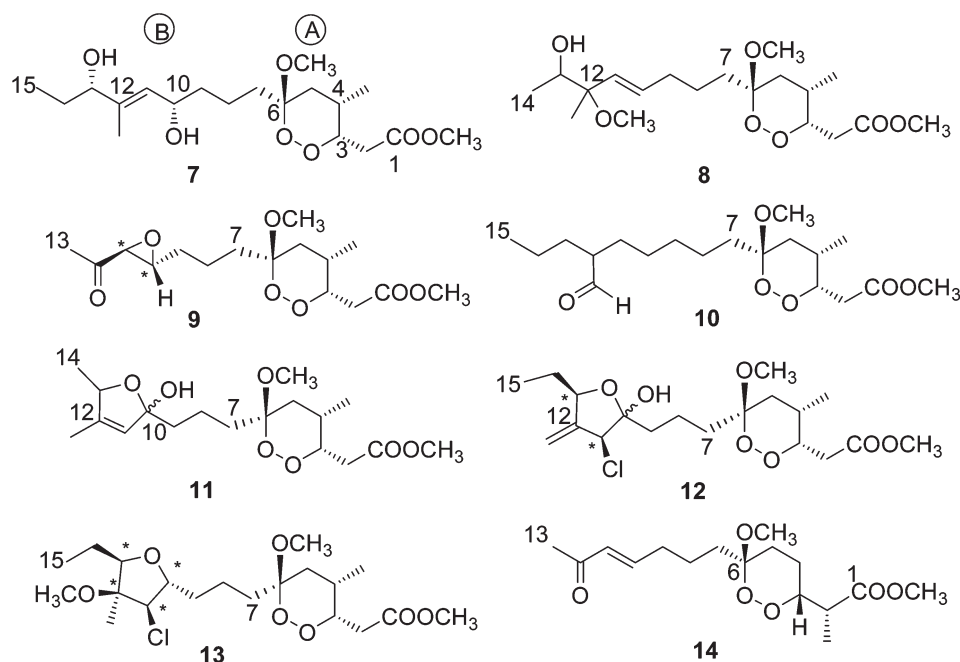
7198 | *Org. Biomol. Chem.*, 2012, **10**, 7197–7207

This journal is © The Royal Society of Chemistry 2012

Fig. 2 Chemical structures of the new compounds manadoperoxides E–K (**7–13**) and peroxyplakoric ester C (**14**). Asterisks indicate that the configuration of the moiety is relative.

Compounds **7–14** have been subjected to a detailed spectrometric (ESI-MS) and spectroscopic (mainly 1D and 2D NMR) analysis, which allowed the definition of their stereostructures (Fig. 2) and the complete assignment of NMR resonances (Tables 1 and 2 or Experimental section). In particular, the NMR analysis revealed that both the ^{13}C NMR resonances from C-1 to C-6, including 4-Me and 6-OMe (moiety A), and the ^1H NMR resonances and coupling constants from H_2-2 to H_2-5 were practically identical within the entire series of compounds **3–5** and **7–13**. This spectroscopic evidence clearly indicated that the new compounds **7–13** must share with the co-occurring manadoperoxides B–D (**3–5**) the structure of the six-membered dioxygenated ring, including the relative configuration at the stereogenic carbons present in this moiety (2D NMR ROESY cross-peaks fully supported this stereochemical assignment). Since we have previously assigned the absolute configuration at all the stereogenic carbons of manadoperoxides A–D (**2–5**) through chemical derivatization and application of the Mosher's method,[17] it is biosynthetically reasonable to assume that the configurations at C-3, C-4 and C-6 reported for compounds **7–13** in Fig. 2 are also the absolute ones. Thus, the new compounds **7–13** differ from manadoperoxides A–D exclusively by the structure of the long ("western") side chain (moiety B) and we will here describe in detail only the determination of this part of their structures.

Manadoperoxide E (**7**) was isolated as a colorless amorphous solid with molecular formula $C_{19}H_{34}O_7$, which, taking into account the structure of the dioxane ring, implied that moiety B should have a $C_{10}H_{19}O_2$ composition and include a single unsaturation degree. The ^1H and ^{13}C NMR spectra of **7** (Experimental section), analyzed with the help of COSY and HSQC data, revealed the presence of two spin systems which closely paralleled those present in the structure of manadoperoxide D (**5**). In particular, the first spin system, from H_2-7 to the sp^2 methine

H-11 (δ_H 5.45, δ_C 127.1) with an oxymethine at H-10 (δ_H 4.40, δ_C 70.1), is identical to that present in the structure of **5**, while the second spin system included a second oxymethine (H-13) attached to a –CH_2CH_3 moiety. The HMBC cross-peaks of 12-Me with C-11, C-12, and C-13 allowed the connection of the above moieties and defined the gross structure of the side chain (moiety B) for manadoperoxide E, which is a homologue of manadoperoxide D. The ROESY cross-peak of 12-Me with H-10 indicated that also in this case the side chain double bond possessed E geometry. Following the same procedure already applied for manadoperoxide D, we determined the absolute configuration at the two stereogenic carbons C-10 and C-13 of **7** through application of the Riguera method for 1,n-diols.[20] Thus, two aliquots of **7** were allowed to react with R- and S-MTPA chloride obtaining the diesters **7a** and **7b**, respectively. According to the Riguera model,[20] in 1,4 MTPA diesters, the combined shielding of the two auxiliary reagents induces positive $\Delta\delta(S$-$R)$ values for the carbinol protons and for all the protons between them. Thus, the positive $\Delta\delta(S$-$R)$ values measured for protons going from H-9 to H-14 (Fig. 3) indicated a 10S,13S configuration.

The molecular formula of manadoperoxide F (**8**), determined by HR-ESIMS, was identical with that of compound **7**, suggesting the same $C_{10}H_{19}O_2$ composition for the side chain. However, analysis of 1D NMR spectra (Tables 1 and 2), together with 2D COSY and HSQC NMR, showed that the moiety B of **8** significantly differed from that of **7** and included a methoxy group (δ_H 3.17, δ_C 49.3), an sp^3 oxymethine (δ_H 3.60, δ_C 73.6) and two mutually coupled sp^2 methines (δ_H 5.67, δ_C 126.8; δ_H 5.49, δ_C 132.2). The COSY spectrum arranged all the proton multiplets of the side chain of **8** within two spin systems: the first spans from H_2-7 to the double bond $\Delta^{10,11}$ while the second spin system includes only the oxymethine (H-13) coupled with a

Table 1 ^{1}H NMR (500 MHz) data of compounds **8–10** and **12–13** in CDCl$_3$

Pos.	8 δ_H, mult. (J in Hz)	9 δ_H, mult. (J in Hz)	10 δ_H, mult. (J in Hz)	12 δ_H, mult. (J in Hz)	13 δ_H, mult. (J in Hz)
2a	2.91, dd (15.6, 9.5)	2.92, dd (15.5, 9.4)	2.92, dd (15.5, 9.5)	2.92, dd (15.7, 9.5)	2.94, dd (15.6, 9.4)
2b	2.52, dd (15.6, 4.2)	2.43, dd (15.5, 4.5)	2.43, dd (15.5, 3.8)	2.42, dd (15.7, 3.5)	2.44, dd (15.6, 3.8)
3	4.37, ddd (9.5, 4.2, 3.0)	4.46, ddd (9.4, 4.5, 3.0)	4.46, ddd (9.5, 3.8, 3.0)	4.44, ddd (9.5, 3.5, 3.0)	4.44, ddd (9.4, 3.8, 3.0)
4	2.50, m	2.57, m	2.56, m	2.57, m	2.57, m
5a	1.68, dd (13.3, 4.3)	1.68^a	1.71^a	1.70^a	1.70^a
5b	1.39^a	1.30^a	1.32^a	1.32^a	1.31^a
7a	1.66^a	1.63^a	1.58^a	1.69^a	1.59^a
7b	1.62^a	1.60^a	1.55^a	1.32^a	1.55^a
8a	1.46, m	1.53, m	1.30^a	1.26^a	1.44^a
8b	1.46, m	1.47, m			1.32^a
9a	2.14, q (7.1)	1.76, m	1.32^a	1.53^a	1.72^a
9b		1.59^a		1.30^a	1.51^a
10	5.67, dt (15.9, 7.1)	3.08, m	1.24^a		3.92, m
11	5.49, d (15.9)	3.20, d (1.7)	1.68^a	4.55, bs	3.50, d (7.4)
12			2.50, m		
13a	3.60, q (6.4)	2.08, s	1.66^a	4.30, t (7.3)	3.74, t (7.3)
13b			1.41^a		
14a	1.08, d (6.4)		1.33^a	2.19, dq (14.2, 7.1)	1.50^a
14b				1.97, m	1.33^a
15			0.88, t (7.0)	1.00, t (7.1)	1.02, t (7.2)
4-Me	0.87, d (7.0)	0.87, d (7.1)	0.85, d (7.0)	0.84, d (7.0)	0.85, d (7.0)
12-Me	1.20, s	3.73, s	9.79, d (2.5)	5.10, bs	1.25, s
1-OMe	3.71, s	3.27, s	3.73, s	5.29, bs	3.73, s
6-OMe	3.23, s		3.28, s	3.73, s	3.28, s
12-OMe	3.17, s			3.28, s	3.33, s

^{a} Overlapped with other signals.

Table 2 ^{13}C NMR data (125 MHz) of compounds **8–10** and **12–13** in CDCl$_3$

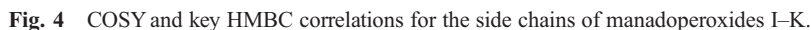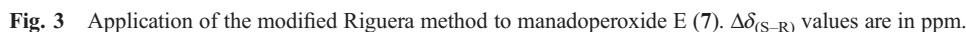| Pos.	8 δ_C, mult.	9 δ_H, mult.	10 δ_H, mult.	12 δ_H, mult.	13 δ_H, mult.
1	173.0, s	172.4, s	171.9, s	171.9, s	172.3, s
2	31.0, t	31.2, t	31.1, t	30.9, t	30.8, t
3	80.1, d	79.9, d	80.1, d	79.6, d	80.3, d
4	27.2, d	27.4, d	26.9, d	26.9, d	27.1, d
5	34.2, t	34.6, t	33.9, t	34.0, t	34.6, t
6	103.7, s	102.8, s	103.0, s	102.8, s	103.1, s
7	32.4, t	32.0, t	32.1, t	33.5, t	33.2, t
8	23.4, t	22.5, t	21.8, t	23.5, t	22.8, t
9	32.6, t	36.5, t	30.1, t	30.0, t	30.8, t
10	126.8, d	57.6, d	28.7, t	116.2, s	79.0, d
11	132.2, d	59.5, d	32.2, t	59.7, d	68.2, d
12	80.7, s	205.8, s	43.5, d	141.6, s	82.4, s
13	73.6, d	24.6, q	32.0, t	83.7, d	84.3, d
14	16.6, q		22.8, t	26.1, t	25.5, t
15			14.2, q	10.4, q	17.0, q
4-Me	16.0, q	16.3, q	16.9, q	17.0, q	17.3, q
12-Me	14.3, q	52.0, q	201.1, d	105.6, t	14.0, q
1-OMe	52.3, q	48.5, q	51.7, q	52.0, q	51.9, q
6-OMe	47.7, q		48.5, q	48.5, q	48.4, q
12-OMe	49.3, q				53.1, q

methyl doublet (Me-14). The HMBC cross-peaks of the methyl singlet at δ_H 1.20 (12-Me) with C-11 and the oxygenated C-12 (δ_C 80.7) and C-13 (δ_C 73.6) and of the methoxy protons with C-12, determined the connection for the above moieties, thus defining the planar structure of the side chain of manadoperoxide F as shown in Fig. 2. The value of $J_{\text{H-10,H-11}}$ = 15.9 Hz indicated the E geometry of Δ;[10] while, due to the very small amounts of manadoperoxide F isolated (∼1.0 mg), needed for

pharmacological evaluation, we could not attempt any determination of the configuration at the two stereogenic carbons of the side chain.

The molecular formula of manadoperoxide G (**9**) (C$_{16}$H$_{26}$O$_7$) was indicative of a C$_7$H$_{11}$O$_2$ side chain, implying two unsaturation degrees. ^{1}H and ^{13}C NMR data of **9** (Tables 1 and 2), analyzed with the help of the 2D HSQC spectrum, sorted out the seven carbon atoms of this moiety as three methylenes, two methines resonating at δ_H 3.08 and 3.20, one methyl singlet (δ_H 2.08) and a ketone carbonyl (δ_C 205.8). The 2D NMR COSY spectrum grouped all the proton multiplets of the side chain in a single spin system terminating with the oxymethines H-10 and H-11. The relatively high field ^{13}C NMR resonances of C-10 and C-11 (δ_C 57.6 and 59.5, respectively) were strongly suggestive of the presence of an epoxide group, which also accounted for the remaining unsaturation degree.

The 2D HMBC cross-peaks of the methyl singlet at δ_H 2.08 with the ketone carbonyl (C-12) and with the epoxide carbon C-11 allowed the connection between the two moieties and the definition of the planar structure of manadoperoxide G (**9**), which can be viewed as an epoxidated manadoperoxide C (**4**). The ROESY correlation between H-11 (δ_H 3.20) and H$_2$-9 indicated the *trans* orientation of the epoxide protons. It should be noted that this relative configuration at C-10 and C-11 has not been connected with that of the remaining stereogenic carbons of the molecule.

Manadoperoxide H (**10**), C$_{19}$H$_{34}$O$_6$ by HR-ESIMS, should possess a C$_{10}$H$_{19}$O composition for moiety B. The presence of an aldehyde carbonyl was suggested by the NMR resonances at δ_H 9.79 and δ_C 201.1 (associated by means of the 2D HSQC spectrum), and this group accounted for the single oxygen atom

7200 | *Org. Biomol. Chem.*, 2012, **10**, 7197–7207

This journal is © The Royal Society of Chemistry 2012

Fig. 3 Application of the modified Riguera method to manadoperoxide E (**7**). $\Delta\delta_{(S-R)}$ values are in ppm.

Fig. 4 COSY and key HMBC correlations for the side chains of manadoperoxides I–K.

and the single unsaturation degree implied for the side chain. Accordingly, the 2D COSY spectrum revealed the presence of a single spin system spanning from H$_2$-7 to Me-15 (δ_H 0.88, t) and including a methine resonating at δ_H 2.50 (H-12) coupled to the doublet at δ_H 9.79. Thus, the aldehyde group should be attached at C-12, as further confirmed by its HMBC cross-peaks with C-11, C-12 and C-13. The configuration at the stereogenic C-12 has been left undetermined.

Manadoperoxide I (**11**) was found to have the molecular formula C$_{18}$H$_{30}$O$_7$ by HR-ESIMS, thus implying a C$_9$H$_{15}$O$_2$ side chain with two unsaturation degrees. Analysis of ^{1}H and ^{13}C NMR spectra (C$_6$D$_6$, see Experimental) of **11**, guided by the 2D HSQC spectrum, revealed the presence of an sp^2 methine singlet (δ_H 5.24, δ_C 122.7), an sp^3 oxymethine (δ_H 4.19, δ_C 77.6) and an hemiketal carbon resonating at δ_C 102.1. In the COSY spectrum, two spin systems (highlighted in bold in Fig. 4) were visible: the first includes a sequence of three methylenes, while the second encompasses only the oxymethine proton coupled to a methyl group. The HMBC cross-peaks of H$_2$-9 with the hemiketal carbon C-10 and with the sp^2 methine C-11 and those of the allylic methyl singlet 12-Me with C-11, C-12 and with the oxymethine C-13 provided the information needed to link the above moieties. Moreover, the HMBC cross-peak H-13/C-10 indicated the presence of the oxygen bridge between C-13 and C-10, thus accounting for the remaining unsaturation degree and completing the gross structure of manadoperoxide I (**11**). A series of signals attributable to a minor compound were detectable both in ^{1}H and ^{13}C NMR spectra of **11** and all our initial attempts to further purify compound **11** failed. However, once the structure of manadoperoxide I was disclosed, these signals were easily rationalized with the presence of an equilibrating mixture (*ca.* 4 : 1 ratio) of the two epimers at C-10. Selected ^{1}H NMR resonances of the minor epimer have been reported in the Experimental section.

Manadoperoxide J (**12**), C$_{19}$H$_{31}$ClO$_7$ by HR-ESIMS, was demonstrated to share with manadoperoxide I (**11**) the presence of an oxygenated five-membered ring and an hemiketal functionality at C-10, in the moiety B. Accordingly, also in this case we observed the presence of an equilibrating mixture (*ca.* 4 : 1 ratio) of the two epimers at C-10. A detailed analysis of ^{1}H and ^{13}C NMR data of the major epimer of **12** (Tables 1 and 2, respectively), aided by 2D NMR spectra, revealed that manadoperoxide J (**12**) actually differs from manadoperoxide I (**11**) by possessing: (i) an ethyl group attached at the oxygenated C-13 (see the COSY cross-peaks shown in Fig. 4) in place of the methyl group; (ii) an sp^2 methylene (δ_H 5.29 and 5.10, δ_C 105.6) instead of the allylic methyl group (iii) a chlorine-bearing sp^3 methine (δ_H 4.55, δ_C 59.7) instead of the sp^2 methine. The 2D HMBC cross-peaks shown by H$_2$-9 (with C-10 and C-11) and by the hexomethylene protons (with C-11, C-12 and C-13), together with the cross-peak H-13/C-10, proved to be crucial to join these moieties as indicated in Fig. 4. The ROESY cross-peak H-11/H-13 revealed the *cis* relative orientation of these protons, but it was not possible to connect this relative configuration with that of the stereogenic carbons of the dioxane ring.

Manadoperoxide K (**13**), C$_{20}$H$_{35}$ClO$_7$ by HR-ESIMS, should possess a C$_{11}$H$_{20}$ClO$_2$ side chain with a single unsaturation degree. The ^{1}H NMR spectrum of **13** (Table 1) revealed, in addition to the signals of moiety A, the resonances of a third methoxy group (δ_H 3.33) and of three methines (δ_H 3.92, 3.50 and 3.74) in the midfield region of the spectrum. All the proton signals were associated to those of the directly linked carbon atoms by means of a 2D HSQC experiment, and then inspection of the 2D COSY experiment disclosed the existence of two spin systems, shown in bold in Fig. 4. The first spin system spans from H$_2$-7 to the chlorine-bearing methine H-11 (δ_H 3.50, δ_C 68.2) and includes the oxymethine at δ_H 3.92 (δ_C 79.0). The second spin system spans from the oxymethine H-13 (δ_H 3.74)

This journal is © The Royal Society of Chemistry 2012

Org. Biomol. Chem., 2012, **10**, 7197–7207 | 7201

to methyl triplet Me-15. The remaining unprotonated carbon atom (δ_C 82.4) present in the ^{13}C NMR spectrum of **13** was attributed to a methoxy-bearing carbon (C-12) located between the two above described moieties on the basis of the $^{2,3}J_{C,H}$ HMBC cross-peaks of the methyl singlet at δ_H 1.24 with C-12, C-11 and C-13 and of the cross-peak of the methoxy group (12-OMe) with C-12. The presence of an ether bridge between C-10 and C-13 to define a THF-type ring was inferred by the HMBC cross-peak H-13/C-10 and accounted for the single unsaturation degree present in the side chain of **13**. This THF-ring includes four stereogenic carbons, whose relative configuration was deduced by the ROESY cross-peaks 12-Me/H$_2$-9, 12-Me/H-11, H-11/H-13, and H$_2$-9/H-13. As for compounds **9** and **12**, this relative configuration has not been connected with that of the stereogenic carbons of the dioxane ring.

Peroxyplakoric ester C (**14**), C$_{17}$H$_{28}$O$_6$ by HR-ESIMS, proved to belong to the structural series of peroxyplakoric esters,[19] which differ from manadoperoxides by the substituents attached at positions 2 and 4 of the dioxane ring (see Fig. 1). A detailed analysis of its ^{1}H and ^{13}C NMR spectra (see Experimental section), accomplished by inspection of 2D COSY and HSQC NMR spectra, revealed that compound **14** shared with peroxy-plakoric ester B$_3$ (**6**)[19] all the carbon and proton resonances, along with the proton–proton coupling constants, for the positions C-1 to C-6 (including also 2-Me and 6-OMe). On the other hand, ^{1}H and ^{13}C NMR resonances of the side chain of **14** were practically superimposable to those of manadoperoxide C (**4**), including an α,β-unsaturated ketone group (δ_C 198.7). The 2D HMBC spectrum provided key information to support these assignments and to join the above partial moieties, thus fully confirming the structure of peroxyplakoric ester C (**14**).

Thus, analysis of the organic extract of *P.* cfr. *lita* afforded twelve endoperoxyketal-containing compounds, eight of which are being described for the first time. These compounds, with the exception of **6** and **14**, share the same stereostructure of the dioxane ring while they differ by the length and/or the functionalization of the "western" side chain. Recently, Garson and co-workers have reported the isolation of a series of dioxane derivatives from the sponge *Plakinastrella clathrata* differing by modifications in the side chain,[21] evidencing the existence of an extraordinary enzymatic activity in Plakinidae sponges, especially dedicated to the functionalization of side chains. However, some of the metabolites isolated in the course of this study are unique in many extents: three of them show the formation of an unprecedented five-membered oxygenated ring which, in two cases, bears also a chlorine atom. To the best of our knowledge this has never been reported for marine endoperoxides.

2.2 Antiprotozoal activity

The library of endoperoxide derivatives obtained from the chemical investigation of *P.* cfr. *lita* have been evaluated *in vitro* for their antiprotozoal activity against *Trypanosoma brucei rhodesiense* and *Leishmania donovani*. Results are reported in Table 3.

Some of the tested compounds showed an ultrapotent activity against *T. b. rhodesiense* at low ng mL^{-1} range. In particular,

Table 3 *In vitro* antiprotozoal activity (IC$_{50}$) and calculated log$P$ values of compounds **3–6**, **8–11**, and **13–14**[a]

Compounds	*T. b. rhodesiense*	*L. donovani*	log$P$[b]
Manadoperoxide B (**3**)	0.003	0.589	4.84
Manadoperoxide C (**4**)	0.678	3.24	2.52
Manadoperoxide D (**5**)	36.7	19.2	2.33
Peroxyplakoric ester B$_3$ (**6**)	3.61	12.0	4.53
Manadoperoxide F (**8**)	0.792	5.73	2.82
Manadoperoxide G (**9**)	1.84	3.22	1.75
Manadoperoxide H (**10**)	0.375	2.44	4.25
Manadoperoxide I (**11**)	0.062	0.633	3.00
Manadoperoxide K (**13**)	0.087	1.89	3.63
Peroxyplakoric ester C (**14**)	30.9	43.4	2.55
Reference compound	0.003[c]	0.174[d]	—

[a] IC$_{50}$ values are in µg mL^{-1} and mean values from at least two replicates (the variation is max. 20%). [b] Calculated by Virtual Computational Chemistry Laboratory software. [c] Melarsoprol. [d] Miltefosine.

manadoperoxide B (**3**) (IC$_{50}$ = 3 ng mL^{-1}) proved to be as active as the reference compound and, to our knowledge, it can be viewed as the most potent trypanocidal marine natural product reported to date. Also remarkably active agents are manadoperoxides I (**11**) and K (**13**) (IC$_{50}$ = 60–90 ng mL^{-1}) and manadoperoxides H (**10**), C (**4**) and F (**8**) (IC$_{50}$ = 300–800 ng mL^{-1}), although their potencies are, respectively, about 30 and 200 times lower than that of manadoperoxide B. The remaining manadoperoxides and the two peroxyplakoric esters proved to be much less active, with IC$_{50}$s in the low–medium µg mL^{-1} range. The tested compounds displayed moderate to good activity against *L. donovani*. The most active compounds of the series were manadoperoxide B (IC$_{50}$ = 0.589 µg mL^{-1}) and manadoperoxide I (IC$_{50}$ = 0.633 µg mL^{-1}) with comparable activities to the reference compound miltefosine (IC$_{50}$ = 0.174 µg mL^{-1}). The remaining compounds showed activity in the µg mL^{-1} range. All the test compounds proved to be non-toxic (IC$_{50}$ >10 µg mL^{-1}) towards the human cell line HMEC-1 (human microvascular endothelial cell line, data not shown). The calculated partition coefficient (log$P$) values of tested metabolites vary between 1.75 to 4.84 (Table 3), hence they comply with Lipinski's rule of five.[22] This also indicates that manadoperoxides will be able to penetrate through lipid cellular membranes and potentially through the blood brain barrier (BBB), which is critical for the treatment of cerebral stage of *Trypanosoma* infections.

3. Discussion

As part of our ongoing screening of natural sources to find new antiprotozoal lead compounds,[7–15] we have now discovered that the endoperoxyketal derivatives manadoperoxides constitute a new class of potent antitrypanosomal agents. The structural variability present within the library of endoperoxides tested in this study clearly defines some structure–activity relationships.

The comparison of the activities of manadoperoxides with those of the closely related peroxyplakoric esters provides valuable information. Indeed, in addition to a negligible difference in the side chain, manadoperoxide B (**3**) and peroxyplakoric ester
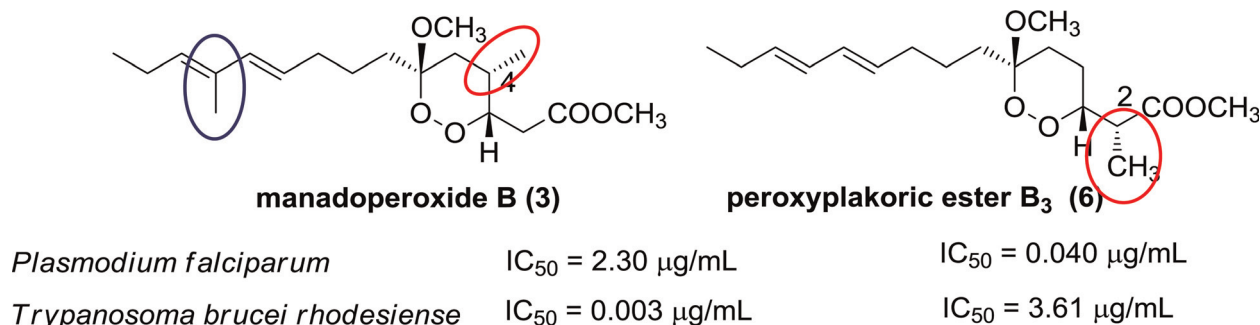
7202 | *Org. Biomol. Chem.*, 2012, **10**, 7197–7207

This journal is © The Royal Society of Chemistry 2012

Fig. 5 Comparison of the structures and the antiprotozoal activities of manadoperoxide B (**3**) and peroxyplakoric ester B$_3$ (**6**).

B$_3$ (**6**) differ only by the position of a methyl group on the ring moiety. In **3** a methyl group is present on the dioxane ring (at C-4), while in **6** it is attached on the short ester-containing side chain (at C-2) (Fig. 5). Interestingly, this minor structural difference is able to induce dramatic effects both in the antimalarial and in the antitrypanosomal activities, but in opposite directions. Indeed, while **6** has been demonstrated to be about 60-fold more active as an antimalarial agent,[17] manadoperoxide B (**3**) is more than 1000-fold more potent as an antitrypanosomal agent. This trend is fully supported by the antitrypanosomal activity of manadoperoxide C (**4**, IC$_{50}$ = 0.678 μg mL^{-1}) (Fig. 1) and peroxyplakoric ester C (**14**, IC$_{50}$ = 30.9 μg mL^{-1}) (Fig. 2). These two compounds share the same structure of the "western" side chain and, thus, they differ exclusively by the shift of a methyl group from C-4 (in **4**) to C-2 (in **14**). As observed for the pair **3**/**6**, this structural change induces a marked reduction of the antitrypanosomal activity in **14**.

These results seem to exclude a non-specific antiprotozoal activity for these peroxyketal derivatives, strongly suggesting their molecular interaction with a defined target(s). In this regard, our studies on plakortin derivatives provided indications about the mechanism of the antimalarial action of simple 1,2-dioxanes[13] which, upon reaction with Fe(II) (most likely the heme iron), should generate an oxygen radical, simultaneously transferred to a side chain carbon. The so formed C-centered radical should then represent the toxic species responsible for the antimalarial activity. In the case of manadoperoxides and peroxyplakoric esters we already demonstrated that the different pattern of substitution around the dioxane ring can induce different conformational preferences of this ring and, consequently, different accessibilities for the interaction with heme iron.[17] Intriguingly, the situation for the antitrypanosomal activity seems to be completely different. In this case, the different pattern of substitution around the dioxane ring and the consequent different conformational behaviour appear to play in favour of the antitrypanosomal activity of manadoperoxides. It is also interesting to notice that the above data suggest, indirectly, that the target(s) of these endoperoxyketal compounds might be different in the two different protozoan parasites.

The complete homogeneity of the stereostructure of the dioxane ring (moiety A) in the series of manadoperoxides B–K can allow a clear evaluation of the impact on the trypanocidal activity of modifications on the alkyl side chain (moiety B). The most active compound of the series, manadoperoxide B (**3**), shows a methyl branched C$_9$ side chain including a conjugated diene system, while the least active compound is manadoperoxide D (**5**), where the presence of a diol group provokes an almost complete loss of activity. The negative effects of an increase in the side chain polarity is fully supported by the trend of activities measured for the other manadoperoxides. Manadoperoxides I (**11**) and K (**13**), bearing a five-membered ring in the side chain, retain very good antitrypanosomal activity, while the carbonyl-containing manadoperoxides H (**10**, saturated C$_9$ alkyl chain with an aldehyde group in place of the methyl group) and C (**4**, conjugated ketone group in side chain) evidence an about 100-fold lower activity compared to manadoperoxide B. An even lower activity was exhibited by manadoperoxides F (**8**, hydroxy group in side chain) and G (**9**, epoxy-ketone group in side chain).

An almost linear relationship between the antitrypanosomal activity and the lipophilicity of the moiety B is clearly indicated by the log$P$ values calculated for the members of the manadoperoxide series (Table 3). This relationship suggests that this moiety is probably not directly involved in the interaction with the target(s), but is responsible for the pharmacokinetic behaviour of these compounds, thus modulating their activities.

Manadoperoxides represent the first endoperoxide derivatives bearing a ketal functionality on the dioxane ring to be evaluated against *Trypanosoma*. A comparison with data available in the literature for the antitrypanosomal activity of related 1,2-dioxanes seems to indicate a positive effect for the alkoxy group at C-6. Indeed, all the natural[23] and synthetic[24] analogues showing an ethyl group or an hydrogen atom in place of the methoxy group at C-6 proved to be less active than manadoperoxides. However, an unambiguous evaluation of this relationship is prevented by the differences in the side chain structures.

Endoperoxide-containing compounds have been reported to target several protozoan parasites and to be potential lead compounds against different tropical diseases. However, while some members of this class show a broad spectrum activity against *Plasmodium*, *Trypanosoma*, *Leishmania*, *etc.*, other endoperoxide-bearing derivatives show a specific action against selected protozoa. Probably the most remarkable example of this second type of antiprotozoal agents is given by artemisinin, a well known antimalarial compound (activity against *P. falciparum* in the low nM range),[25] displaying a very modest activity (about 25 μg mL^{-1}) against *T. b. rhodesiense*.[25] As we have shown before, peroxyplakoric ester B$_3$ (**6**) and its analogue **14** follow the same behaviour as artemisinin. On the other hand, manadoperoxides show an opposite behaviour, possessing moderate
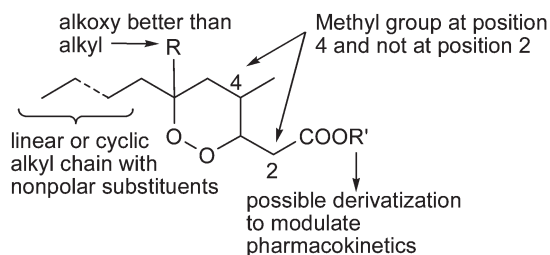
Fig. 6 Schematic view of the structure–activity relationships for anti-trypanosomal 1,2-dioxanes.

activity against *Plasmodium falciparum* (3–10 μM), which is *ca.* 1000 times lower than the trypanocidal activity described herein (Fig. 5).

Since the cell organization and the biochemical composition of trypanosomes differ in numerous aspects from those of mammalian cells, several parasite-specific processes may provide selective targets for drug development and, among these, purine salvage, fatty acid elongation, cytochrome-independent oxidase and trypanothione reductase have been suggested.[26,27] This latter flavoenzyme is of key importance to maintain the redox balance within the parasite acting as regulator of the levels of trypanothione, a molecule composed by glutathione and spermidine and involved in the reduction of hydroperoxides and ribonucleotides.[27] Although a shortage of material prevented us from investigating the mechanism of action of manadoperoxides, an interference with the finely regulated redox balance within the parasite could be anticipated.

The analysis of our library of natural compounds and comparison with data available in the literature have demonstrated unambiguously that the endoperoxy group does not confer *per se* activity against *Trypanosoma* (and other protozoan parasites responsible for tropical diseases), while the contribution of the carbon skeleton is of pivotal importance. We have summarized in Fig. 6 the most important structural requirements for the class of simple 1,2-dioxanes as they have emerged from the present study.

4. Experimental section

4.1 General experimental procedures

Low and high resolution ESI-MS spectra were performed on a LTQ OrbitrapXL (Thermo Scientific) mass spectrometer. ^{1}H (500 MHz) and ^{13}C (125 MHz) NMR spectra were measured on Varian INOVA spectrometers. Chemical shifts were referenced to the residual solvent signal (CDCl$_3$: δ_H 7.26, δ_C 77.0; C$_6$D$_6$: δ_H 7.16, δ_C 128.1). Homonuclear ^{1}H connectivities were determined by the COSY experiment. Through-space ^{1}H connectivities were evidenced using a ROESY experiment with a mixing time of 500 ms. One-bond heteronuclear ^{1}H–^{13}C connectivities were determined by the HSQC experiment; two- and three-bond ^{1}H–^{13}C connectivities by gradient-HMBC experiments optimized for a $^{2,3}J$ of 8 Hz. Medium pressure liquid chromatography was performed on a Büchi apparatus using a silica gel (230–400 mesh) column. HPLC were achieved on a Knauer apparatus equipped with a refractive index detector and LUNA

(Phenomenex) SI60 or C18 (250 × 4 mm) columns. The log*P* values of manadoperoxides were estimated using VCCLAB, Virtual Computational Chemistry Laboratory, online server (http://www.vcclab.org).[32]

4.2 Animal material, extraction, isolation

A specimen of *Plakortis lita* de Laubenfels (order Homosclerophorida, family Plakinidae) was collected in January 2010 from along the coasts of the Bunaken island in the Bunaken Marine Park of Manado. A voucher sample (Man/10/02) has been deposited at the Dipartimento di Chimica delle Sostanze Naturali, Università di Napoli Federico II. The sponge is massive, roundish; the colour *in vivo* and in the preserved state is light brown externally and internally. The sponge is very soft and easy to cut, but it contracts after preservation. Surface smooth in the living specimen, but after collection, especially in the dried state, the surface became irregular and wrinkled. Ostia are not detectable on the living specimens. Oscules with a very low rim, about 1.5 mm in diameter. The ectosomal skeleton is an irregular reticulation of rounded or elliptical meshes. In some area a disorganized arrangement of tangential spicules is present. Choanosome with a confused skeleton of scattered spicules. Spicules are straight or bent, thin diods (98 × 2.5 μm on average); rare triods (actines 33 μm on average); irregular strongyloid microrhabds (2.5–25 μm) and smooth ovoid spheres (about 2 μm in diameter). The studied material is very similar to *P. lita* de Laubenfels in the spicular complement, which consists of diods, triods and in irregular strongyloid microrhabds, comparable in size and similar in shape. A skeletal organisation of the ectosome with rounded meshes, typical of *P. lita* de Laubenfels, is also present. This species differs from *P. lita* de Laubenfels by the presence of tangential spicules irregularly arranged, never reported in *P. lita*, and by the colour which in this last species may be black, dark brown, or grey-brown. Spheres, detected in the present material, were not described in *P. lita*. The present sample has been compared also to *Plakortis hooperi* Muricy[18] from Papua New Guinea. *P. hooperi* possesses a spicule complement, comparable to that of the present material, of diods, triods, microrhabds and spheres; it is characterized by a brown colour, similar to that of *P.* cfr. *lita* and by a confused ectosomal skeleton, without trace of reticulation. *P. hooperi* differs from *P.* cfr. *lita* in lacking an ectosomal reticulation of rounded meshes, in the shape and size of the diods, relatively thick and without a well-marked centre, in the shape and size of microrhabds (shorter and irregular in *P. hooperi*), and of the spheres (more spherical and larger). Pending deeper morphological studies, the present sample is provisionally assigned to *P.* cfr. *lita* on the basis of the numerous shared morphological characters.

After homogenization, the organism was exhaustively extracted, in sequence, with methanol and chloroform. The combined organic extracts (8.16 g) were subjected to chromatography over C18 silica column (200–400 mesh) eluting with a solvent gradient of decreasing polarity from water to chloroform. Fractions eluted with H$_2$O–MeOH 2:8 and H$_2$O–MeOH 1:9 were combined (1.35 g) and further fractionated by gravity column chromatography on silica gel using a *n*-hexane–EtOAc gradient. Fractions eluted with *n*-hexane–EtOAc 9:1 were

7204 | *Org. Biomol. Chem.*, 2012, **10**, 7197–7207

This journal is © The Royal Society of Chemistry 2012

subjected to repeated column and HPLC chromatographies (*n*-hexane–EtOAc 95 : 5) affording manadoperoxides B (**3**, 15.1 mg), J (**12**, 0.9 mg) and I (**11**, 1.3 mg) in the pure state. Fractions eluted with *n*-hexane–EtOAc 8 : 2 were re-chromatographed by HPLC (*n*-hexane–EtOAc 8 : 2, flow 0.8 mL min^{-1}) to give manadoperoxide K (**13**, 2.3 mg), F (**8**, 1.1 mg) and G (**9**, 1.3 mg). Fractions eluted with *n*-hexane–EtOAc 7 : 3 were re-chromatographed by HPLC (*n*-hexane–EtOAc 75 : 25) affording pure manadoperoxide C (**4**, 1.1 mg), H (**10**, 1.3 mg) and another fraction, further purified by RP-HPLC (MeOH–H$_2$O 85 : 15, flow 0.8 mL min^{-1}) to yield peroxyplakoric ester C (**14**, 1.3 mg). Fractions eluted with *n*-hexane–EtOAc (1 : 9) were re-chromatographed by RP-HPLC (MeOH–H$_2$O 6 : 4, flow 0.8 mL min^{-1}) affording manadoperoxide D (**5**, 2.1 mg) and E (**7**, 2.5 mg).

4.3 Manadoperoxide E (7)

Colorless amorphous solid; $[\alpha]_D^{25}$ −13.0 (*c* 0.2, CHCl$_3$); ^{1}H NMR (CDCl$_3$, 500 MHz): δ_H 5.45 (1H, d, *J* = 8.7 Hz, H-11), 4.43 (1H, ddd, *J* = 9.5, 4.3, 3.0 Hz, H-3), 4.40 (1H, m, H-10), 4.26 (1H, m, H-13), 3.72 (3H, s, 1-OMe), 3.26 (3H, s, 6-OMe), 2.97 (1H, dd, *J* = 15.5, 9.5 Hz, H-2a), 2.57 (1H, m, H-4), 2.44 (1H, dd, *J* = 15.5, 4.3 Hz, H-2b), 1.71 (3H, bs, H-17), 1.69 (1H, overlapped, H-5a), 1.64 (1H, overlapped, H-9a), 1.62 (1H, overlapped, H-7a), 1.61 (2H, overlapped, H$_2$-14), 1.55 (1H, overlapped, H-9b), 1.42 (1H, overlapped, H-8a), 1.35 (1H, overlapped, H-8b), 1.34 (1H, overlapped, H-7b), 1.00 (3H, t, *J* = 7.1 Hz, Me-15), 0.86 (3H, d, *J* = 7.1 Hz, 4-Me); ^{13}C NMR (CDCl$_3$, 125 MHz) δ_C 172.5 (s, C-1), 142.0 (s, C-12), 127.1 (d, C-11), 103.0 (s, C-6), 79.7 (d, C-3), 73.4 (d, C-13), 70.1 (d, C-10), 52.2 (q, 1-OMe), 48.7 (q, 6-OMe), 38.4 (t, C-9), 34.5 (t, C-5), 31.7 (t, C-2), 31.4 (t, C-7), 27.9 (t, C-14), 27.2 (d, C-4), 22.0 (t, C-8), 17.0 (q, C-7), 10.1 (q, C-15). (+) ESI-MS *m/z* 375 [M + H]$^+$, 397 [M + Na]$^+$. HR-ESIMS (positive ions): found *m/z* 397.2200, C$_{19}$H$_{34}$NaO$_7$ requires *m/z* 397.2202.

4.4 Reaction of manadoperoxide E (7) with *R*- and *S*-MTPA chloride

Compound **7** (1.0 mg, 2.8 μmol) was treated with *R*-MTPA chloride (30 μL) in 400 μL of dry pyridine with a catalytic amount of DMAP overnight at rt. Then, the solvent was removed and the product was purified by HPLC (*n*-hexane–EtOAc, 97 : 3) to obtain the *S*-MTPA diester **7a** (1.2 mg, 60% yield). When compound **7** (1.0 mg, 2.8 μmol) was treated with *S*-MTPA chloride, following the same procedure, 1.5 mg (69% yield) of *R*-MTPA diester **7b** was obtained. *S*-MTPA diester **7a**: amorphous solid; ESI-MS (positive ions) *m/z* 807 [M + H]$^+$; ^{1}H NMR (CDCl$_3$): selected values δ 5.61 (1H, m, H-10), 5.45 (1H, d, *J* = 8.7 Hz, H-11), 5.43 (1H, m, H-13), 1.77 (3H, s, 12-Me), 1.60 (1H, m, H-9a), 1.55 (2H, m, H-7), 1.40 (1H, m, H-9b), 1.64 (2H, overlapped, H$_2$-14). *R*-MTPA diester **7b**: amorphous solid; ESI-MS (positive ions) *m/z* 807 [M + H]$^+$; ^{1}H NMR (CDCl$_3$): selected values δ 5.59 (1H, m, H-10), 5.43 (1H, d, *J* = 8.7 Hz, H-11), 5.38 (1H, m, H-13), 4.37 (1H, m, H-3), 1.75 (3H, s, 12-Me), 1.59 (1H, m, H-9a), 1.55 (2H, m, H-7), 1.39 (1H, m, H-9b), 1.62 (2H, overlapped, H$_2$-14).

4.5 Manadoperoxide F (8)

Colorless amorphous solid; $[\alpha]_D^{25}$ −12.1 (*c* 0.1, CHCl$_3$); ^{1}H NMR (CDCl$_3$, 500 MHz): Table 1; ^{13}C NMR (CDCl$_3$, 125 MHz): Table 2; (+) ESI-MS *m/z* 375 [M + H]$^+$, 397 [M + Na]$^+$. HR-ESIMS (positive ions): found *m/z* 397.2197, C$_{19}$H$_{34}$NaO$_7$ requires *m/z* 397.2202.

4.6 Manadoperoxide G (9)

Colorless amorphous solid; $[\alpha]_D^{25}$ −13.5 (*c* 0.2, CHCl$_3$); ^{1}H NMR (CDCl$_3$, 500 MHz): Table 1; ^{13}C NMR (CDCl$_3$, 125 MHz): Table 2; (+) ESI-MS *m/z* 331 [M + H]$^+$, 353 [M + Na]$^+$. HR-ESIMS (positive ions): found *m/z* 353.1510; C$_{16}$H$_{26}$NaO$_7$ requires *m/z* 353.1506.

4.7 Manadoperoxide H (10)

Colorless amorphous solid; $[\alpha]_D^{25}$ −18.1 (*c* 0.1, CHCl$_3$); ^{1}H NMR (CDCl$_3$, 500 MHz): Table 1; ^{13}C NMR (CDCl$_3$, 125 MHz): Table 2; (+) ESI-MS *m/z* 359 [M + H]$^+$, 381 [M + Na]$^+$. HR-ESIMS (positive ions): found *m/z* 381.2259; C$_{19}$H$_{34}$NaO$_6$ requires *m/z* 381.2253.

4.8 Manadoperoxide I (11)

Colorless amorphous solid; $[\alpha]_D^{25}$ −19.3 (*c* 0.1, CHCl$_3$); ^{1}H NMR (C$_6$D$_6$, 500 MHz): δ_H 5.24 (1H, bs, H-11), 4.50 (1H, m, H-3), 4.19 (1H, q, *J* = 6.9 Hz, H-13), 3.34 (3H, s, 1-OMe), 3.20 (3H, s, 6-OMe), 2.88 (1H, dd, *J* = 15.5, 9.3 Hz, H-2a), 2.50 (1H, m, H-4), 2.14 (1H, dd, *J* = 15.5, 4.4 Hz, H-2b), 1.68 (1H, m, H-7a), 1.66 (1H, m, H-9a), 1.62 (1H, m, H-9b), 1.59 (1H, m, H-7b), 1.44 (1H, overlapped, H-5a), 1.38 (1H, m, H-8a), 1.36 (3H, bs, 12-Me), 1.33 (1H, m, H-8b), 1.17 (3H, d, *J* = 6.9 Hz, Me-14), 0.88 (1H, overlapped, H-5b), 0.38 (3H, d, *J* = 7.0 Hz 4-Me); ^{1}H NMR data for the minor epimer (only resonances differing from those of the major epimer are reported): δ_H 4.15 (1H, q, *J* = 6.9 Hz, H-13), 1.19 (3H, d, *J* = 6.9 Hz, H-14), 1.69 (1H, m, H-9a), 1.58 (1H, m, H-9b); ^{13}C NMR (C$_6$D$_6$, 125 MHz): δ_C 171.8 (s, C-1), 135.8 (s, C-12), 122.7 (d, C-11), 102.9 (s, C-6), 102.1 (s, C-10), 79.7 (d, C-3), 77.6 (d, C-13), 52.2 (q, 1-OMe), 48.8 (q, 6-OMe), 40.8 (t, C-9), 34.3 (t, C-5), 33.8 (C-7), 31.7 (t, C-2), 27.1 (d, C-4), 22.5 (t, C-8); 18.5 (q, C-14), 17.2 (q, 12-Me), 15.8 (q, 4-Me); (+) ESI-MS: *m/z* 359 [M + H]$^+$, 381 [M + Na]$^+$. HR-ESIMS (positive ions): found *m/z* 381.1892; C$_{18}$H$_{30}$NaO$_7$ requires *m/z* 381.1889.

4.9 Manadoperoxide J (12)

Colorless amorphous solid; $[\alpha]_D^{25}$ −11.9 (*c* 0.1, CHCl$_3$); ^{1}H NMR (CDCl$_3$, 500 MHz): Table 1; ^{1}H NMR data for the minor epimer (only resonances differing from those of the major epimer are reported): δ_H 4.55 (1H, bs, H-11), 4.38 (1H, m, H-13), 1.78 (1H, overlapped, H-14a), 1.56 (1H, overlapped, H-14b), 1.00 (3H, t, *J* = 7.0 Hz, H-15); ^{13}C NMR (CDCl$_3$, 125 MHz): Table 2; (+) ESI-MS *m/z* 407 and 409 (about 3 : 1 ratio) [M + H]$^+$, 429, 431 (about 3 : 1 ratio) [M + Na]$^+$.

HR-ESIMS found *m/z* 429.1663; $C_{19}H_{31}^{35}ClNaO_7$ requires *m/z* 429.1656.

4.10 Manadoperoxide K (13)

Colorless amorphous solid; $[\alpha]_D^{25}$ −11.5 (*c* 0.3, CHCl₃); ¹H NMR (CDCl₃, 500 MHz): Table 1; ¹³C NMR (CDCl₃, 125 MHz): Table 2; (+) ESI-MS: *m/z* 423 and 425 (about 3 : 1 ratio) [M + H]⁺, 445 and 447 (about 3 : 1 ratio) [M + Na]⁺. HR-ESIMS (positive ions): found *m/z* 445.1972; $C_{20}H_{35}^{35}ClNaO_7$ requires *m/z* 445.1969.

4.11 Peroxyplakoric ester C (14)

Colorless amorphous solid; $[\alpha]_D^{25}$ −3.0 (*c* 0.3, CHCl₃); ¹H NMR (CDCl₃, 500 MHz): δ_H 6.77 (1H, dt, *J* = 16.5, 6.5 Hz, H-10), 6.18 (1H, d, *J* = 16.5 Hz, H-11), 4.19 (1H, m, H-3), 3.75 (3H, s, 1-OMe), 3.27 (3H, s, 6-OMe), 3.07 (1H, dq, *J* = 9.5, 7.0 Hz, H-2), 2.25 (2H, m, H₂-9), 2.24 (3H, s, Me-13), 2.10 (1H, m, H-4a), 1.75 (1H, m, H-5a), 1.69 (1H, m, H-7a), 1.65 (1H, m, H-5b), 1.53 (2H, m, H₂-8), 1.40 (1H, m, H-4b), 1.30 (1H, m, H-7b), 1.12 (3H, d, *J* = 7.0 Hz, 2-Me); ¹³C NMR (CDCl₃, 125 MHz): δ_C 198.7 (s, C-12), 172.5 (s, C-1), 147.0 (d, C-10), 132.1 (d, C-11), 104.5 (s, C-6), 81.0 (d, C-3), 52.0 (q, 1-OMe), 48.8 (6-OMe), 41.6 (t, C-2), 32.9 (t, C-7), 32.6 (t, C-9), 27.3 (q, C-13), 26.5 (t, C-5), 21.8 (t, C-8), 20.5 (t, C-4), 17.0 (q, 2-Me). (+) ESI-MS *m/z* 351 [M + Na]⁺. HR-ESIMS (positive ions): found *m/z* 351.1790, $C_{17}H_{28}NaO_6$ requires *m/z* 351.1784.

4.12 Activity against *Trypanosoma brucei rhodesiense*

Minimum Essential Medium (50 μL) supplemented with 25 mM HEPES, 1 g L⁻¹ additional glucose, 1% MEM non-essential amino acids (100×), 0.2 mM 2-mercaptoethanol, 1 mM Na-pyruvate and 15% heat inactivated horse serum was added to each well of a 96-well microtitre plate. Serial drug dilutions of eleven 3-fold dilution steps covering a range from 100 to 0.002 μg mL⁻¹ were prepared. Then 10⁴ bloodstream forms of STIB 900 strain of *T. b. rhodesiense* in 50 μL was added to each well and the plate incubated at 37 °C under a 5% CO₂ atmosphere for 72 h. 10 μL of a resazurin solution (12.5 mg resazurin dissolved in 100 mL double-distilled water) was then added to each well and incubation continued for a further 2–4 h. Then the plates were read in a Spectramax Gemini XS microplate fluorometer (Molecular Devices Cooperation, Sunnyvale, CA, USA) using an excitation wavelength of 536 nm and an emission wavelength of 588 nm. The IC₅₀ values were calculated by linear regression (Huber 1993)[33] from the sigmoidal dose inhibition curves using SoftmaxPro software (Molecular Devices Cooperation, Sunnyvale, CA, USA). Melarsoprol was the standard drug.

4.13 Activity against *Leishmania donovani*

Amastigotes of *L. donovani* (strain MHOM/ET/67/L82) were grown in axenic culture at 37 °C in SM medium at pH 5.4 supplemented with 10% heat-inactivated fetal bovine serum under an atmosphere of 5% CO₂ in air. One hundred μL of culture medium with 10⁵ amastigotes from axenic culture with or without a serial drug dilution were seeded in 96-well microtitre plates. Serial drug dilutions covering a range from 90 to 0.001 μg mL⁻¹ were prepared. After 72 h of incubation the plates were inspected under an inverted microscope to assure growth of the controls and sterile conditions. 10 μL of a resazurin solution (12.5 mg resazurin dissolved in 100 mL double-distilled water) was then added to each well and the plates incubated for another 2 h. Then the plates were read in a Spectramax Gemini XS microplate fluorometer using an excitation wavelength of 536 nm and an emission wavelength of 588 nm. Data were analyzed using the software Softmax Pro. Decrease of fluorescence (*i.e.* inhibition) was expressed as percentage of the fluorescence of control cultures and plotted against the drug concentrations. The IC₅₀ values were calculated from the sigmoidal inhibition curves. Miltefosine was used as a reference drug.

4.14 Cell cytotoxicity assay

HMEC-1 cell line immortalized by SV 40 large T antigen was maintained in MCDB 131 medium supplemented with 10% fetal calf serum, 10 ng ml⁻¹ of epidermal growth factor, 1 μg ml⁻¹ of hydrocortisone, 2 mM glutamine, 100 U ml⁻¹ of penicillin, 100 μg ml⁻¹ of streptomycin, and 20 mM Hepes buffer. Cells were treated with serial dilutions of test compounds and cell proliferation evaluated using the MTT (3-(4,5-dimethylthiazol-2-yl)-2,5-diphenyltetrazolium bromide) assay.[15]

Conclusions

In the last decade, the urgent need for viable alternatives to the existing antiquated and unsatisfactory therapeutic options has stimulated a remarkable increase in the efforts towards finding new antitrypanosomal agents, often as a result of a series of public–private partnerships. A number of different classes of active compounds have been proposed and, among them, purine nitriles,[28] thiosemicarbazones,[29] quinolones,[30] and chalcone–benzoxaborole[31] appear to display better trypanocidal potential and better selectivity. Somewhat surprisingly, in spite of the incredible chemical diversity associated with the secondary metabolites elaborated by terrestrial plants and marine invertebrates, the contribution of natural products chemistry to the fight against trypanosomiasis has been until now modest. As matter of fact, the above reported classes of recently developed trypanocidal compounds include only synthetically produced molecules.

Data presented in this paper have disclosed that manadoperoxides constitute one of the most potent classes of natural products acting against sleeping sickness isolated to date and strongly suggest that endoperoxyketal-containing molecules are of promise for further development as lead structures against African trypanosomiasis. Moreover, the structure–activity relationships deduced have revealed that minor structural changes around the dioxane ring can dramatically affect the pharmacological activity, thus suggesting the interaction of this moiety with a specific target(s).

Since trypanosomiasis affects the poorest countries, the cost of the treatment is one of the main concerns in the design of new chemotherapeutics and, although effective, too expensive drugs

7206 | *Org. Biomol. Chem.*, 2012, **10**, 7197–7207

This journal is © The Royal Society of Chemistry 2012

should be discarded. In this regard, the natural product state of manadoperoxides should not be considered as a drawback on the way to their development as antitrypanosomal drugs; indeed their relatively simple structures should guarantee the feasibility of a total synthesis. They are small, lipophilic and appear to have good pharmacokinetic properties, so they offer significant drug-likeness to become bioavailable lead compounds. A number of syntheses of the six-membered endoperoxyketal scaffold have been already published in the literature, very recently also by our group.[15] These should allow the preparation of large libraries of compounds and the development of this new class of antitrypanosomal agents.

Acknowledgements

References

1 C. Burri, S. Nkunku, A. Merolle, T. Smith, J. Blum and R. Brun, *Lancet*, 2000, **355**, 1419–1425.
2 E. M. Fèvre, B. V. Wissmann, S. C. Welburn and P. Lutumba, *PLoS Negl. Trop. Dis.*, 2008, **2**, e333.
3 N. M. El-Sayed, P. J. Myler and D. C. Bartholomeu, *Science*, 2005, **309**, 409–415.
4 M. P. Barrett, I. M. Vincent, R. J. S. Burchmore, A. J. N. Kazibwe and E. Matovu, *Fut. Microbiol.*, 2011, **6**, 1037–1047.
5 P. G. Kennedy, *Ann. Neurol.*, 2008, **64**, 116–126.
6 http://www.dndi.org/portfolio/fexinidazole.html
7 E. Fattorusso, S. Parapini, C. Campagnuolo, N. Basilico, O. Taglialatela-Scafati and D. Taramelli, *J. Antimicrob. Chemother.*, 2002, **50**, 883–888.
8 G. Chianese, S. R. Yerbanga, L. Lucantoni, A. Habluetzel, N. Basilico, D. Taramelli, E. Fattorusso and O. Taglialatela-Scafati, *J. Nat. Prod.*, 2010, **73**, 1448–1452.
9 F. Scala, E. Fattorusso, M. Menna, O. Taglialatela-Scafati, M. Tierney, M. Kaiser and D. Tasdemir, *Mar. Drugs*, 2010, **8**, 2162–2174.
10 C. Campagnuolo, E. Fattorusso, A. Romano, O. Taglialatela-Scafati, N. Basilico, S. Parapini and D. Taramelli, *Eur. J. Org. Chem.*, 2005, 5077–5083.
11 E. Fattorusso, O. Taglialatela-Scafati, A. Ianaro and M. Di Rosa, *Tetrahedron*, 2000, **56**, 7959–7967.
12 C. Fattorusso, G. Campiani, B. Catalanotti, M. Persico, N. Basilico, S. Parapini, D. Taramelli, C. Campagnuolo, E. Fattorusso, A. Romano and O. Taglialatela-Scafati, *J. Med. Chem.*, 2006, **49**, 7088–7094.
13 O. Taglialatela-Scafati, E. Fattorusso, A. Romano, F. Scala, V. Barone, P. Cimino, E. Stendardo, B. Catalanotti, M. Persico and C. Fattorusso, *Org. Biomol. Chem.*, 2010, **8**, 846–856.
14 C. Fattorusso, M. Persico, N. Basilico, D. Taramelli, E. Fattorusso, F. Scala and O. Taglialatela, *Bioorg. Med. Chem.*, 2011, **19**, 312–320.
15 M. Persico, A. Quintavalla, F. Rondinelli, C. Trombini, M. Lombardo, C. Fattorusso, V. Azzarito, D. Taramelli, S. Parapini, Y. Corbett, G. Chianese, E. Fattorusso and O. Taglialatela-Scafati, *J. Med. Chem.*, 2011, **54**, 8526–8540.
16 In our paper cited in ref. 17 this sponge was tentatively attributed to *Plakortis* cfr. *simplex* on the basis of its morphological relationships with the *Plakortis simplex* species complex. However, on the basis of a comparison with the detailed morphological data later published (ref. 18), we consider conspecific the specimens analyzed both in this study and in our previous work (ref. 17) and attribute them to the species *Plakortis* cfr. *lita*.
17 C. Fattorusso, M. Persico, B. Calcinai, C. Cerrano, S. Parapini, D. Taramelli, E. Novellino, A. Romano, F. Scala, E. Fattorusso and O. Taglialatela-Scafati, *J. Nat. Prod.*, 2010, **73**, 1138–1145.
18 G. Muricy, *J. Mar. Biol. Assoc. UK*, 2011, **91**, 303–319.
19 M. Kobayashi, K. Kondo and I. Kitagawa, *Chem. Pharm. Bull.*, 1993, **41**, 1324–1326.
20 F. Freire, J. M. Seco, E. Quinoa and R. Riguera, *J. Org. Chem.*, 2005, **70**, 3778–3790.
21 K. W. L. Yong, L. K. Lambert, P. Y. Hayes, J. J. De Voss and M. J. Garson, *J. Nat. Prod.*, 2012, **75**, 351–360.
22 C. A. Lipinski, F. Lombardo, B. W. Dominy and P. J. Feeney, *Adv. Drug Delivery Rev.*, 2001, **46**, 3–26.
23 M. H Kossuga, A. M. Nascimento, J. Q. Reimao, A. G. Tempone, N. N. Taniwaki, K. Veloso, A. G. Ferreira, B. C. Cavalcanti, C. Pessoa, M. O. Moraes, A. M. S. Mayer, E. Haidu and R. G. S. Berlinck, *J. Nat. Prod.*, 2008, **71**, 334–339.
24 H. Holla, M. Labaied, N. Phom, I. D. Jenkins, K. Stuart and R. J. Quinn, *Bioorg. Med. Chem. Lett.*, 2011, **21**, 4793–4797.
25 M. Kaiser, S. Wittlin, A. Nehrbass-Stuedli, Y. Dong, X. Wang, A. Hemphill, H. Matile, R. Brun and J. L. Vennerstrom, *Antimicrob. Agents Chemother.*, 2007, **51**, 2991–2993.
26 A. Cavalli and M. L. Bolognesi, *J. Med. Chem.*, 2009, **52**, 7339–7359.
27 R. L. Krauth-Siegel, H. Bauer and R. H. Schirmer, *Angew. Chem., Int. Ed.*, 2005, **44**, 690–715.
28 Z. Qiao, Q. Wang, F. Zhang, Z. Wang, T. Bowling, B. Nare, R. T. Jacobs, J. Zhang, D. Ding, Y. Liu and H. Zhou, *J. Med. Chem.*, 2012, **55**, 3553–3557.
29 J. P. Mallari, A. A. Shelat, T. Obrien, C. R. Caffrey, A. Kosinski, M. Connelly, M. Harbut, D. Greenbaum, J. H. McKerrow and R. K. Guy, *J. Med. Chem.*, 2008, **51**, 545–552.
30 J. P. Mallari, A. A. Shelat, A. Kosinski, C. R. Caffrey, M. Connelly, F. Zhu, J. H. McKerrow and R. K. Guy, *Bioorg. Med. Chem. Lett.*, 2008, **18**, 2883–2885.
31 G. Hiltensperger, N. G. Jones, S. Niedermeier, A. Stich, M. Kaiser, J. Jung, S. Puhl, A. Damme, H. Braunschweig, L. Meinel, M. Engstler and U. Holzgrabe, *J. Med. Chem.*, 2012, **55**, 2538–2548.
32 I. V. Tetko, J. Gasteiger, R. Todeschini, A. Mauri, D. Livingstone, P. Ertl, V. A. Palyulin, E. V. Radchenko, N. S. Zefirov, A. S. Makarenko, V. Y. Tanchuk and V. V. Prokopenko, *J. Comput. Aided Mol. Des.*, 2005, **19**, 453–463.
33 W. Huber and J. C. Koella, *Acta Trop.*, 1993, **55**, 257–261.